Pergamon

Int. J. Multiphase Flow Vol. 24, No. 2, pp. 189–212, 1998

Printed in Great Britain
PII: S0301-9322(97)00056-6
0301-9322/98 $19.00 + 0.00

HEAT TRANSFER IN INTERMITTENT AIR–WATER FLOWS—PART II

UPWARD INCLINED TUBE

G. HETSRONI, J. H. YI, B. G. HU, A. MOSYAK, L. P. YARIN and G. ZISKIND
Faculty of Mechanical Engineering, Technion—Israel Institute of Technology, Haifa 32000, Israel

(Received 6 January 1997; in revised form 28 July 1997)

Abstract—This paper presents a study on the heat transfer in intermittent air–water flows in an upward inclined tube. The experimental technique is based on infrared thermography of an electrically heated wall of the tube, providing both visualization of the temperature field and measurements of the local wall temperature. Local heat transfer coefficients and flow parameters have been measured for air–water flow in a pipe of 49.2 mm inner diameter at inclination angles of 2° and 5°. The water and air Froude numbers varied from 0.59 to 2.0 and from 0.03 to 0.57, respectively. Experimental correlations of the heat transfer coefficient indicate that the liquid and gas Froude numbers and dimensionless frequency of bubble appearance are good correlating parameters. A simple physical model was developed to correlate between the flow parameters and the heat transfer. © 1998 Elsevier Science Ltd. All rights reserved

Key Words: air–water flow, inclined tube, thermography, heat transfer

1. INTRODUCTION

Gas–liquid two-phase flow in inclined tubes is widely encountered in many important technical applications: solar collectors, chemical plants, nuclear reactors, oil wells and pipelines, evaporators, condensers, etc. A knowledge of the two-phase heat transfer coefficient is very important in safety considerations, since a slug or intermittent flow is accompanied by oscillations in pipe temperature which, in fact, may be more damaging than a high absolute temperature.

Many investigators have studied the hydrodynamics of two-phase flow and attempted to define the boundaries between various flow regimes. Some of the available flow pattern data are for an inclined tube. Zukoski (1966) investigated experimentally the influence of the viscosity and surface tension on bubble velocity for different tube inclination angles. In particular, the combined effects of surface tension and inclination angle were demonstrated. Data obtained by Barnea *et al.* (1980) for flow patterns in tubes with inclination in the range from −10° to 10° show a dramatic change of the flow pattern at inclination angle of 0.25°. The effect of the small upward inclination angles was systematically investigated by conducting a series of air–water tests at upward inclination angles of 1/2, 2 and 7° (Weisman and Kang 1981).

Heat transfer in inclined tubes is of major importance for some practical applications. Solar thermal electricity is one of the most extensively employed ways of using renewable energies in the world. The state-of-the-art of Solar Thermal Power Plants is marked by more than 2.5 million square meters of parabolic-trough collectors installed in the nine plants currently in operation in California. The plants use oil as the heat transfer fluid between the solar field and the power block connected to the external grid. This thermal fluid has to be at 400°C, to achieve high thermal efficiency of the steam power cycle. Only synthetic oils are available for this purpose, and these oils are expensive and dangerous. A program was started to replace the thermal oil by water, which is directly heated and evaporated in the tubes of parabolic-trough solar collectors, producing steam at temperatures of above 400°C and pressures of around 100 bar. This is the so-called Direct Steam Generation (DSG) Technology.

The available scientific knowledge on two-phase flow phenomena and flow stability in DSG technology does not cover the ranges of geometrical and operational parameters valid for

advanced parabolic-trough solar fields. In contrast to conventional evaporators, the process inside the absorber pipe is characterized by

- slightly upward inclined two-phase flow;
- large pipe diameters (typically ~5 cm) and low flow velocities;
- non-uniform and transient heat flux to the pipe wall.

Due to low flow velocities and due to the inclination of the pipe, evaporation occurs in the intermittent flow regime. Stratified flow may cause strongly non-uniform cooling and bending of the pipes. It is known from theory (Barnea and Taitel 1986) and experimental investigations (Muller 1993) that for given inlet conditions, diameter, inclination and heat flux, a minimum mass flow rate is required to avoid stratified flow.

A few experimental studies on flow boiling in inclined tubes are found in the literature. Bogdanov (1955) used water flowing in a tube ($D = 20$ mm) inclined at 45°, Gilli (1963) used tubes with $D = 15$ mm and 23 mm at 15° inclination, Krishna and Rao (1985) found that in bubbly or intermittent flow the heat transfer coefficient passed through a minimum with increasing angle of inclination. One can see that in these studies pipe diameters were small; thus, the results cannot be applied to the DSG technology.

The studies on tubes of larger diameters are usually restricted to the adiabatic case. Only few studies of the application of adiabatic correlations to non-adiabatic water/steam flows in slightly inclined pipes were reported before the experimental investigations by Muller (1995) and Creutz (1994), Creutz *et al.* (1995).

Heat transfer to non-boiling two-phase flows is also widely used in industrial processes. In non-boiling systems, the enhancement of convective heat transfer by injecting a gas-phase in confined liquid flows in vertical tubes has been observed. The experimental data from Dorresteijn (1970) show that the heat transfer coefficients increase with increasing flow velocities. Elamvaluthi and Srinivas (1984) performed an experimental investigation of two-phase two-component vertical flows in pipes. The heat transfer in inclined tubes received comparatively little attention from researchers.

The aim of the present work is to investigate the parameters of an air–water flow and heat transfer mechanism in inclined tubes of relatively large diameters, and to explain the experimental findings by an adequate theoretical model. The experiments in a non-boiling flow allow us to observe wavy structures, and to measure wave velocity and frequency. The expected detailed knowledge will refer to bubble length, height, frequency and velocity, depending on flow rates and pipe inclination. On this basis, the local heat transfer into the pipe will be studied, depending on the flow pattern and pipe inclination. Knowledge of the local heat transfer coefficient and its dependence on the actual flow pattern should yield a better understanding of the coupling between the heat transfer and two-phase flow.

2. EXPERIMENTAL CONDITIONS

The experimental data were collected for the single-phase water and two-phase air–water heat transfer, and for the bubble motion parameters. Experiments were performed for the inclination angles $\beta = 2.0°$ and 5.0°, and for various water and air superficial velocities in an elongated bubble with dispersed bubble flow regime. The experiments were carried out in the range of gas superficial velocities $0.02 \leq U_{GS} \leq 0.39$ m/s and water superficial velocities $0.40 \leq U_{LS} \leq 1.4$ m/s. The Froude number range was $0.03 \leq Fr_G \leq 0.57$, $0.59 \leq Fr_L \leq 2.0$, where $Fr_G = U_{GS}/(gD)^{0.5}$, $Fr_L = U_{LS}/(gD)^{0.5}$, g is the acceleration due to gravity.

The experimental technique used in all the experiments was the same as that for the study of heat transfer phenomena in a horizontal tube. In all cases the uncertainty of reported data does not differ from that calculated from experiments in the horizontal tube. The experimental conditions are given in table 1.

In figure 1, our data for an inclination of +5° are plotted in the flow pattern map given by Taitel and Dukler (1976). According to this map, the intermittent regime may be divided into three subregions denoted as elongated bubble (EB), characterized by a laminar flow in the liquid slug and long transient bubble trails; elongated bubble with dispersed bubble (EB + DB),

Table 1. Experimental conditions

Inclination angle β (deg)	Superficial liquid velocity U_{LS} (m/s)	Superficial gas velocity U_{GS} (m/s)
2.0	0.40	0.020, 0.13
	0.82	0.056, 0.23
	1.40	0.090, 0.39
5.0	0.40	0.020, 0.056, 0.090, 0.13, 0.17, 0.23, 0.31
	0.82	0.39
	1.40	

characterized by the onset of a turbulent flow in the liquid and subsequent appearance of dispersed bubbles in the liquid; and finally, slug flow (SL), the region in which the gas fraction in the liquid slug exceeds 10%.

As shown in figure 1, experiments were carried out in EB + DB regime. The flow pattern is similar to that in a horizontal tube, but the dispersed bubbles are much smaller. The mechanism of heat transfer is quite different for horizontal and inclined tubes, and we will give a framework for an analysis of the effect of the fluid motion on the heat transfer in these two cases.

3. PHYSICAL MODEL OF HEAT TRANSFER ON THE UPPER PART OF THE TUBE SURFACE

Two-phase bubble flow is commonly defined as a flow in which gas-phase is distributed within liquid continuum. In order to predict the heat transfer in horizontal and inclined pipes, it is important to elucidate the turbulent structure of the continuous liquid-phase. Knowing this structure, one can address the contribution of bubbles to the flow characteristics. As a first step toward the understanding of the local heat transfer mechanisms, we propose to subdivide the heat transfer phenomenon in the intermittent flow into two components: one due to the liquid turbulence, and the other due to effects caused by the bubble motion.

For horizontal and inclined pipes an elongated gas bubble is in the upper part of the pipe. Intermittent flow consists of liquid slugs and gas bubbles which are usually greater in length than one pipe diameter. The liquid may or may not contain dispersed bubbles, depending on

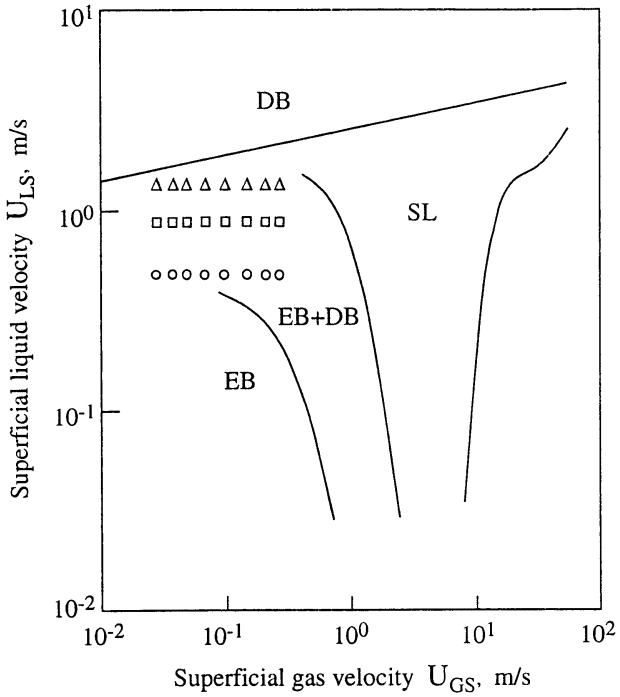

Figure 1. Flow regime map at inclination angle $\beta = 5°$: DB, dispersed bubble flow; EB, elongated bubble flow; SL, slug flow – ○, $U_{LS} = 0.4$ m/s; □, $U_{LS} = 0.82$ m/s; △, $U_{LS} = 1.4$ m/s.

Table 2. Heat transfer coefficient at the top of the tube

Superficial liquid velocity U_{LS} (m/s)	Superficial gas velocity U_{GS} (m/s)	Clear water α (W/m^2 K)	Air–water flow			
			$\beta = 2^\circ$ $\alpha_{\theta=0}$	$\beta = 5^\circ$ $\alpha_{\theta=0}$	$\beta = 2^\circ$ $\alpha_{\theta=0}/\alpha$	$\beta = 5^\circ$ $\alpha_{\theta=0}/\alpha$
0.40	0.020	2800	2800	3000	1.00	1.07
	0.056			3200		1.14
	0.090			3200		1.14
	0.13		2850	3400	1.02	1.21
	0.17			3600		1.28
	0.23			3600		1.27
	0.31			3350		1.20
	0.39			3300		1.18
0.82	0.020	4600		4900		1.07
	0.056		4900	5150	1.07	1.12
	0.090			5250		1.14
	0.13			5380		1.17
	0.17			5240		1.14
	0.23		5300	5600	1.15	1.22
	0.31			5450		1.18
	0.39			5650		1.23
1.40	0.020	7000		7400		1.06
	0.056			7400		1.06
	0.090		6790	7200	0.97	1.03
	0.13			7800		1.11
	0.17			8200		1.17
	0.23			8050		1.15
	0.31			8000		1.14
	0.39		8200	8100	1.17	1.16

the gas and liquid flow rates and turbulence level in the slug. In the case of air–water intermittent flow, the average two-phase heat transfer coefficient α on the upper part of the tube will depend on the air-phase heat transfer coefficient α_b, water-phase heat transfer coefficient α_s, heat transfer coefficient of mixture zone α_m, and the time periods $\Delta\tau_s$, $\Delta\tau_b$, $\Delta\tau_m$ it takes for the air-phase, water-phase and mixture zone, respectively to pass a fixed point.

Our analysis concerns the elongated bubble with dispersed bubble regime. An elongated bubble is usually streamlined with a nose and a tail. The tail of the bubble sometimes breaks off from the main body of the bubble and is picked up by the next bubble. As the gas velocity increases, dispersed bubbles start to appear at the leading edge of the slug. The appearance of dispersed bubbles in the slug is associated with the mixing zone.

The time-average air–water two-phase heat transfer coefficient on the upper part of the tube may be written in the following way:

$$\alpha_\theta = \frac{1}{\tau}(\alpha_s\Delta\tau_s + \alpha_b\Delta\tau_b + \alpha_m\Delta\tau_m) \quad [1]$$

where $\tau = \Delta\tau_s + \Delta\tau_b + \Delta\tau_m$ represents the total time for water-phase and air-phase to pass the fixed point.

If the air flow rate is low, the mixture zone is not significant, and [1] can be written as

$$\alpha_\theta = \frac{1}{\tau}(\alpha_s\Delta\tau_s + \alpha_b\Delta\tau_b). \quad [2]$$

If L_i is the bubble length, then $\Delta\tau_b$ is given by

$$\Delta\tau_b = \frac{1}{u_b}\sum_{i=1}^{N} L_i \quad [3]$$

where N is the number of bubbles passing a fixed point during the time period τ. Relation [3] assumes that u_b is independent of L. The validity of this assumption will be shown below.

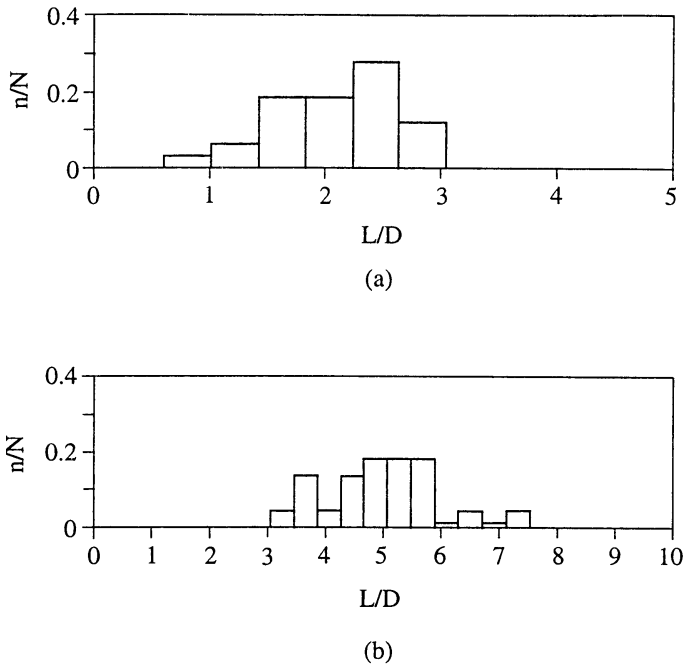

Figure 2. Bubble length distribution at inclination angle $\beta = 2^\circ$ and $Fr_L = 0.59$: (a) $Fr_G = 0.03$; (b) $Fr_G = 0.19$.

Define the bubble average length L and the frequency of bubble appearance f as

$$L = \frac{1}{N}\sum_{i=1}^{N} L_i, \; f = \frac{1}{\tau} N. \qquad [4]$$

From [3] and (4] we obtain:

$$\frac{\Delta\tau_b}{\tau} = \frac{fL}{u_b}. \qquad [5]$$

Using [5] in a dimensionless form, [2] can be expressed as

$$\frac{\alpha_\theta}{\alpha} = \frac{\alpha_s}{\alpha}\left(1 - \frac{fL}{u_b}\right) + \frac{\alpha_b}{\alpha}\frac{fL}{u_b} \qquad [6]$$

where α is the heat transfer coefficient for the liquid single-phase, fL/u_b is the ratio of the time for air bubbles to pass the fixed point to the total time for air- and water-phases, and $(1 - fL/u_b)$ is the ratio of the time for water slugs to pass the fixed point to the total time.

It should be noted that the water-phase heat transfer coefficient α_s may be different from α. The water slugs may contain many dispersed bubbles which will increase the water-phase turbulence level and convection heat transfer coefficient. So-called bubble-induced turbulence may take place in inclined tubes. Therefore, the two-phase heat transfer coefficient depends on air and water physical parameters, and on the interaction between the air- and water-phases.

[6] reflects the relationship between two-phase heat transfer and hydrodynamics. Hence, in the study of the two-phase heat transfer, it is necessary to determine not only the heat transfer coefficient, but also the bubble motion parameters.

4. EXPERIMENTAL RESULTS

In this section, the influence of inclination angle and air and water Froude numbers on bubble size, bubble motion and two-phase heat transfer will be discussed. The experimental data collected are related to the two following groups:

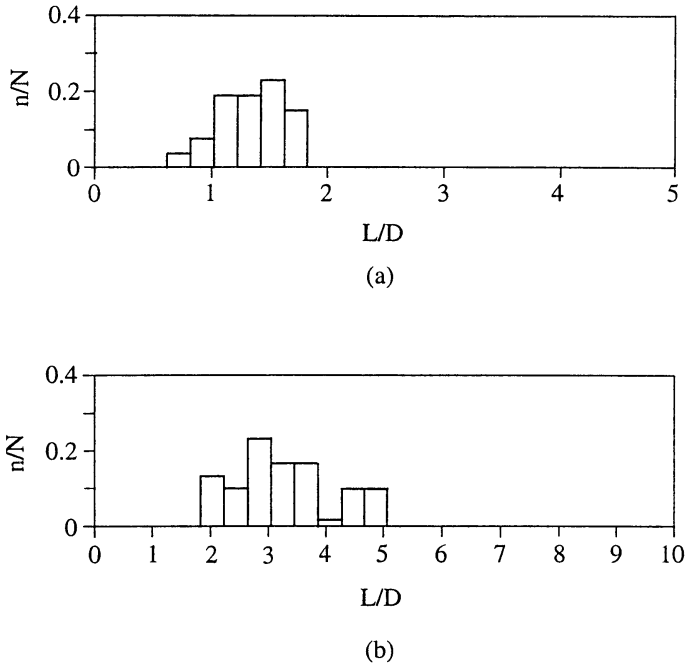

Figure 3. Bubble length distribution at inclination angle $\beta = 5°$ and $Fr_L = 0.59$: (a) $Fr_G = 0.03$; (b) $Fr_G = 0.19$.

1. bubble geometry parameters and bubble motion;
2. heat transfer on the upper and lower surfaces of the pipe.

4.1. *Bubble geometry parameters*

4.1.1. *Bubble length distribution*. Typical dimensionless bubble length spectra for various pipe inclinations, and for various air and water Froude numbers, are presented in figures 2(a,b) and 3(a,b). It can be seen that the bubble length distribution depends on the inclination angle and the air and water Froude numbers. For smaller air and water Froude numbers, the range of bubble length distribution is narrow, i.e. bubbles are uniform in length. With increase in the air Froude number at a constant water flow rate, the range of bubble length distribution becomes wider and the bubbles become longer. Generally, an increase in the air Froude number at a constant water Froude number leads to an increase in the bubble size, especially at low water

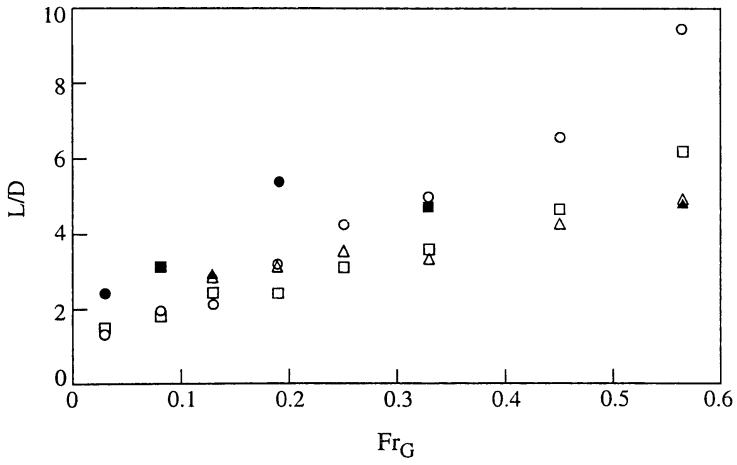

Figure 4. Average dimensionless bubble length: $\beta = 5°$ – ○, $Fr_L = 0.59$; □, $Fr_L = 1.2$; △, $Fr_L = 2.0$; $\beta = 2°$ – ●, $Fr_L = 0.59$; ■, $Fr_L = 1.2$; ▲, $Fr_L = 2.0$.

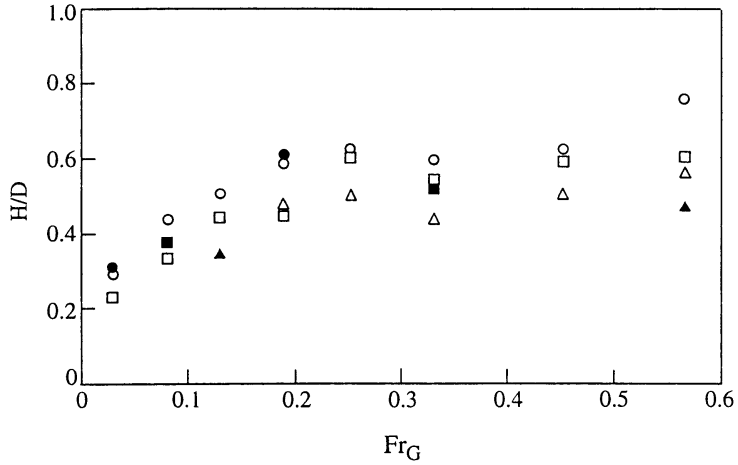

Figure 5. Average dimensionless bubble height: $\beta = 5^\circ$ – ○, $Fr_L = 0.59$; □, $Fr_L = 1.2$; △, $Fr_L = 2.0$; $\beta = 2^\circ$ – ●, $Fr_L = 0.59$; ■, $Fr_L = 1.2$; ▲, $Fr_L = 2.0$.

Froude numbers. With inclination angle decreasing from 5° to 2°, the range of bubble length distribution becomes wider and the bubbles become longer.

4.1.2. *Average dimensionless bubble length and height*. From the bubble length distribution, the average dimensionless bubble length $\bar{L} = L/D$ can be calculated. For various water and air Froude numbers, it is shown in figure 4. For both inclination angles, $\beta = 2^\circ$ and 5°, the average dimensionless bubble length increases when the air Froude number increases at the same water Froude number. Conversely, the bubbles become shorter with water Froude number increasing at the same air Froude number.

Similarly, the average dimensionless bubble height H/D can be calculated from the bubble height distribution.

The effect of water and air Froude numbers on the average dimensionless bubble height is shown in figure 5. For the inclination angles $\beta = 2^\circ$ and 5°, the bubble height increases substantially in the range $0 < Fr_G < 0.2$, and then remains approximately constant.

4.2. *Bubble motion*

4.2.1. *Bubble velocity*. The influence of water and air Froude numbers on the dimensionless bubble velocity $u_b/\sqrt{gD}$ is shown in figure 6. For the inclination angles $\beta = 2^\circ$ and 5°, the bubble velocity increases with an increase in either water or air Froude number.

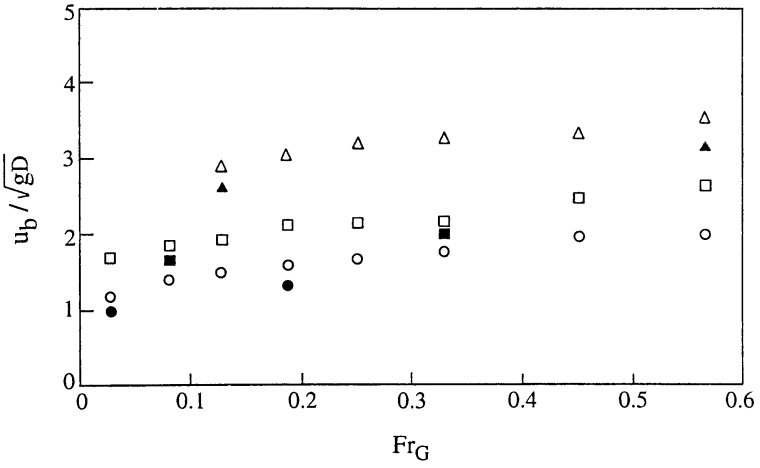

Figure 6. Average dimensionless bubble velocity: $\beta = 5^\circ$ – ○, $Fr_L = 0.59$; □, $Fr_L = 1.2$; △, $Fr_L = 2.0$; $\beta = 2^\circ$ – ●, $Fr_L = 0.59$; ■, $Fr_L = 1.2$; ▲, $Fr_L = 2.0$.

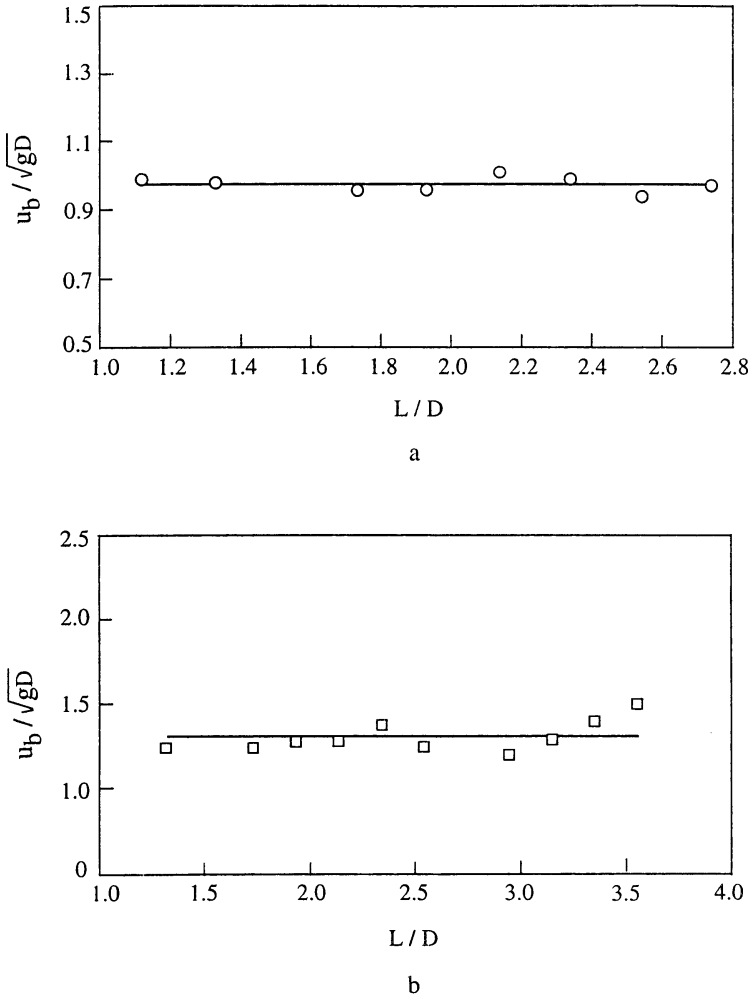

Figure 7. Effect of bubble length on bubble velocity, $\beta = 5°$: (a) $Fr_L = 0.59$, $Fr_G = 0.08$; (b) $Fr_L = 1.2$, $Fr_G = 0.13$.

For $\beta = 5°$, the effect of bubble length on bubble velocity, at two different combinations of liquid and gas Froude numbers, is shown in figure 7(a,b). One can see that u_b is independent of L, as was assumed earlier. In figure 8(a,b) we plotted $u_b/\sqrt{gD}$ vs. the gas Froude number for two different values of the liquid Froude numbers. There is good agreement with the result of Singh and Griffith (1970), shown by a straight line.

4.2.2. *Frequency of bubble appearance*. Figure 9 shows the frequency of bubble appearance vs. the air Froude number for $\beta = 2°$ and $5°$. When the air Froude number is large enough, the bubbles become long and their number decreases, though the bubble velocity increases.

The effect of the water Froude number on the frequency of bubble appearance can also be seen from figure 9. For $\beta = 2°$ and $5°$ at the same air flow rates, the frequency of bubble appearance increases with the water Froude number. This frequency also increases when the inclination angle increases from $2°$ to $5°$, at the same water and air Froude numbers.

In figure 10, the dimensionless parameter fL/u_b is plotted vs. the air Froude number. For both $\beta = 2°$ and $5°$, fL/u_b increases with increasing air Froude number at the same water Froude number. However, it should be noted that for $Fr_L = 1.2$ the experimental value of fL/u_b at $Fr_G = 0.33$ is higher than its values at $Fr_G > 0.33$.

4.3. *Heat transfer on the upper surface*

The main objective of this study is to determine the variation of the heat transfer coefficient from the heated wall to the fluid, and to study the effect of air and water flow rates and incli-

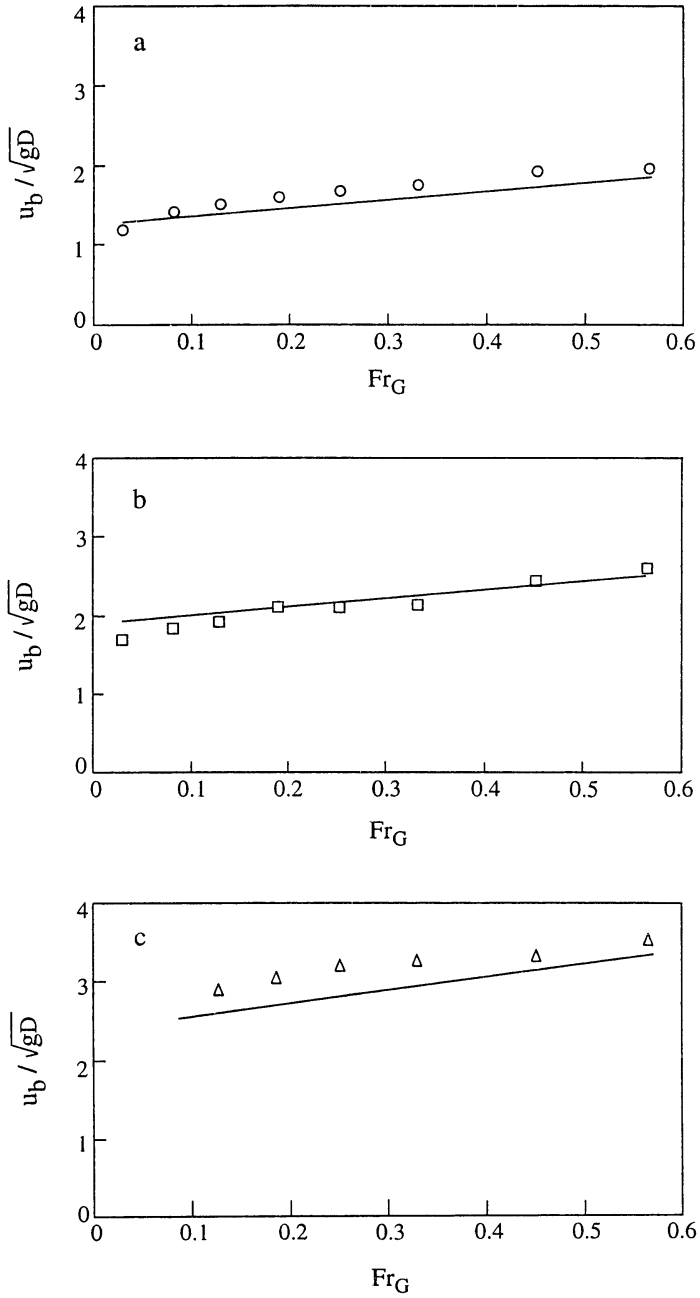

Figure 8. Comparison of the experimental data for (a) $Fr_L = 0.59$, (b) $Fr_L = 1.2$ and calculations of Singh and Griffith (1970, straight line) for bubble velocity at inclination angle $\beta = 5°$.

nation angle on the heat transfer coefficient. The two-phase test series was performed at the range of heat flux q from 27 to 53 kW/m^2. Every test was repeated to check the results.

The main part of the results presented below is related to heat transfer at inclination angle of 5°. We also present some results for $\beta = 2°$.

4.3.1. *Heat transfer coefficient fluctuation on the top of the tube.* Typical heat transfer coefficient fluctuation on the upper part of the tube is presented in figure 11(a) for the clear water, and in figure 11(b) for the air–water mixture at the same superficial liquid velocity ($Fr_L = 0.59$, $Fr_G = 0.45$).

Figure 11(a) shows variation of the heat transfer coefficient in the turbulent flow of water in a pipe. This variation reflects the time-dependent character of the fluctuating features of the flow. The mean value of the coefficient in this case is 2800 ± 150 W/m^2 K. The deviation from the

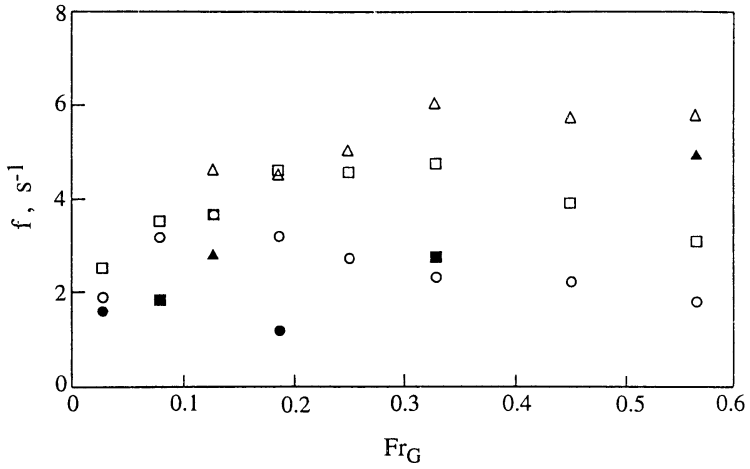

Figure 9. Frequency of bubble appearance: $\beta = 5^\circ$ – ○, $Fr_L = 0.59$; □, $Fr_L = 1.2$; △, $Fr_L = 2.0$; $\beta = 2^\circ$ – ●, $Fr_L = 0.59$; ■, $Fr_L = 1.2$; ▲, $Fr_L = 2.0$.

mean value in this case does not exceed 6%, which is within the limits of accuracy of the present work.

For the air–water flow, the heat transfer coefficient increases to 3350 ± 300 W/m^2 K. In this case, the deviation from the mean value is about 9%. One can note, however, that the maximum deviation reaches ± 650 W/m^2 K, i.e. about 19%. Such behaviour of the heat transfer coefficient reflects the essence of the intermittent flow, which by its nature is non-stationary. In their extensive study, Shoham *et al.* (1982) also observed fluctuations in wall temperature and heat transfer rate with time. The presence of waves induces flow disturbances. These disturbances will grow or decay with time, leading to fluctuations of wave height, fluid pressure, and temperature. Figure 11(b) does not make it possible to determine the frequency of temperature fluctuations. For this purpose, a special method should be developed, as was done by Lin and Hanratty (1987) for pressure fluctuation measurements.

Increase in the air Froude number, at a constant water Froude number, enhances the heat transfer coefficient fluctuation, especially at low water flow rates. This phenomenon may be explained as follows: in an air–water slug system, there is not a continuous-phase on the upper part of the tube, and there exists a large difference between the air-phase heat transfer coefficient and the water-phase one. Thus, the heat transfer coefficient increases when a water slug passes the measuring point, and decreases when an air bubble passes the measuring point.

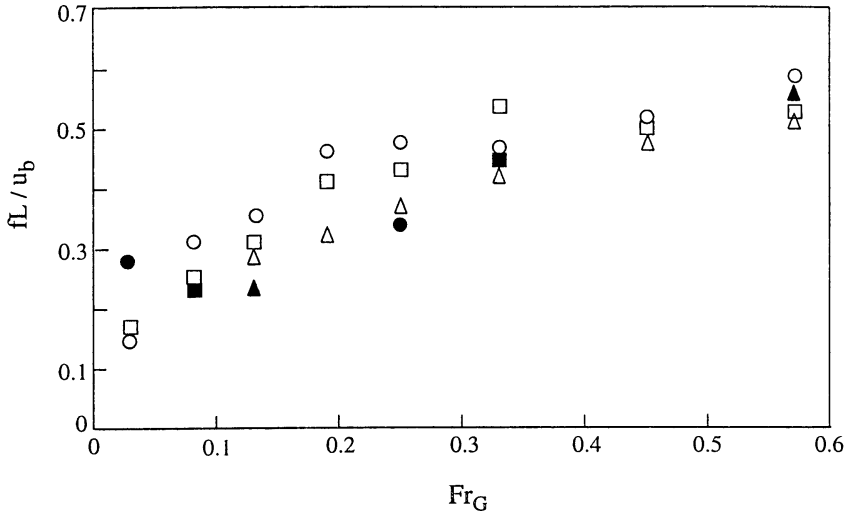

Figure 10. Dependence of fL/u_b on gas Froude number: $\beta = 5^\circ$ – ○, $Fr_L = 0.59$; □, $Fr_L = 1.2$; △, $Fr_L = 2.0$; $\beta = 2^\circ$ – ●, $Fr_L = 0.59$; ■, $Fr_L = 1.2$; ▲, $Fr_L = 2.0$.

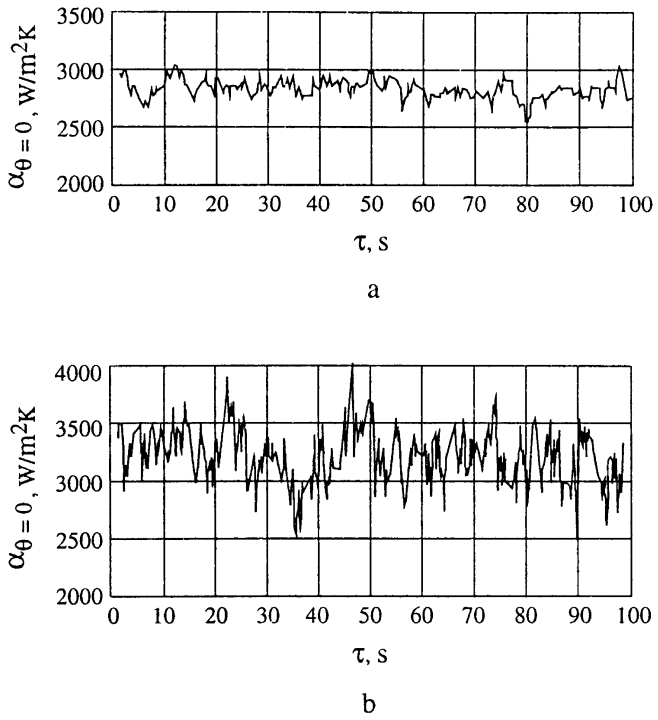

Figure 11. Heat transfer coefficient fluctuation on the top of the tube, $Fr_L = 0.59$: (a) single phase; (b) $Fr_G = 0.45$.

4.3.2. *Time-average dimensionless heat transfer coefficient on the top of the tube, Table 2.* The dimensionless average heat transfer coefficient is defined as

$$\frac{\alpha_{\theta=0}}{\alpha} = \frac{1}{\alpha\tau}\int_0^{\tau} \alpha_{\theta=0}\, d\tau \qquad [7]$$

where α is the heat transfer coefficient for single-water-phase, and $\tau = 300$ s in the present study.

A plot of the time-average dimensionless heat transfer coefficient $\alpha_{\theta=0}/\alpha$ vs. the gas Froude number is given in figure 12. All experimental data may be described by a single curve. This curve shows a small increase in the dimensionless heat transfer coefficient at the range of gas Froude numbers $Fr_G \leq 0.3$; then $\alpha_{\theta=0}/\alpha$ tends to a constant value of about 1.2. The scale of the eddies generated by bubbles depends on bubble size and velocity. An increase in bubble velocity enhances the disturbance in the bubble wake, which acts as a turbulence promoter.

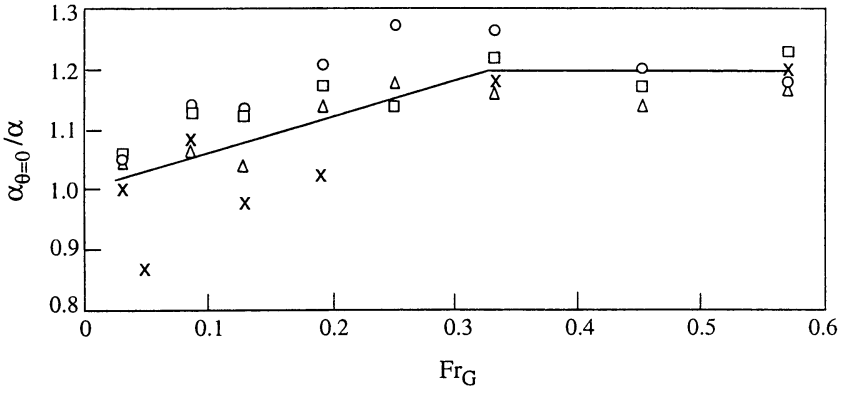

Figure 12. Time-average dimensionless heat transfer coefficient on the top of the tube: $\beta = 5° - \bigcirc$, $Fr_L = 0.59$; □, $Fr_L = 1.2$; △, $Fr_L = 2.0$; $\beta = 2° - \bullet$, $Fr_L = 0.59$; ■, $Fr_L = 1.2$; ▲, $Fr_L = 2.0$.

The time-average heat transfer coefficient is obtained, with a standard deviation of $\pm 8\%$, as:

$$\frac{\alpha_{\theta=0}}{\alpha} = 1 + 0.6\mathrm{Fr_G} \ @ \ 0 \le \mathrm{Fr_G} \le 0.3 \qquad [8]$$

$$\frac{\alpha_{\theta=0}}{\alpha} = 1.2 \ @ \ 0.3 \le Fr_G \le 0.57. \qquad [9]$$

4.3.3. *Phase discrimination and local heat transfer*. When measurements of wall temperature, as well as other techniques, are used to study a two-phase flow, the first important problem is to identify the phases. If these phases are separated (like in a flow with elongated bubbles in a horizontal tube), the problem becomes relatively simple. But it is difficult to handle the phase identification in inclined tubes, since the heat transfer coefficients for gas and liquid are rather similar. In order to solve this problem, many sets of successive temperature fields were studied. Figure 13(a) illustrates a typical temperature field on the heated wall when a bubble passes on the upper part. Figure 13(b) shows the temperature distribution when the liquid-phase passes. The IR radiometer was located 0.8 m above the pipe, and was able to detect temperature changes on the upper side of the heated surface. The flow is from the right to the left, the dimensions are in millimetres, and the colour shades reflect the wall temperature (the red colour corresponds to a higher temperature, the blue one corresponds to a lower temperature). Interesting quantitative features may be observed in figure 13(a,b): when the heating surface is covered with a bubble, the wall temperature decreases (i.e. the colour changes from red to green) if the dimensionless angle $\theta = 2\varphi/\pi$ increases from 0 to 0.17, where φ is the angle from the top of the tube.

When the heating surface is in contact with the liquid, the opposite tendency is observed: the wall temperature increases in the range $\theta \le 0.17$. If $\theta > 0.17$, the wall temperature is almost independent of θ. The bubble length is much larger than the field of view. Figure 13(a,b) shows the instantaneous temperature distributions. One can see that the instantaneous temperature field is not uniform, which reflects the nature of the intermittent flow. Further analysis of the temperature field and measurements of circumferential temperature distribution at $0.17 \le \theta \le 0.8$ show that the wall temperature does not change within this range.

For each angle θ the time-average heat transfer coefficient for the liquid- and gas-phases was calculated as:

$$\alpha_s = \frac{1}{\Delta\tau_s}\int_0^{\Delta\tau_s} \alpha_s \, \mathrm{d}\tau \qquad [10]$$

$$\alpha_b = \frac{1}{\Delta\tau_b}\int_0^{\Delta\tau_b} \alpha_b \, \mathrm{d}\tau. \qquad [11]$$

The instantaneous values of α_b and α_s were calculated from the data provided by the IR radiometer in the line mode. Along the same circumferential line, the values of wall temperature at different θ were obtained. For a given θ, we assume that when the wall temperature retains for some time its almost constant minimum value, there is a water slug over the line, and α_s can be determined. From the instant the temperature begins to increase, and till the moment it returns to the minimum value, there is a bubble over the line, and the data is used to determine α_b.

For a bubble or liquid moving along the heating surface, the characteristic times can be defined from [5) and (6].

Figure 14 shows the time-average dimensionless heat transfer coefficient vs. the angle θ for the case when liquid (white points) or bubble (black points) are in contact with the heating surface. The data for the liquid Froude number $\mathrm{Fr_L} = 0.59$ and gas Froude number $\mathrm{Fr_G} = 0.45$ are presented. This case corresponds to a maximum value of the temperature fluctuation [see figure 11(a,b)]. There is a significant difference between the dimensionless heat transfer coefficients for liquid- and gas-phases, but each of these does not change more than 10% within the angle $0 < \theta \le 0.8$.

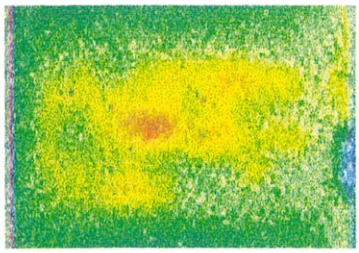

(a)

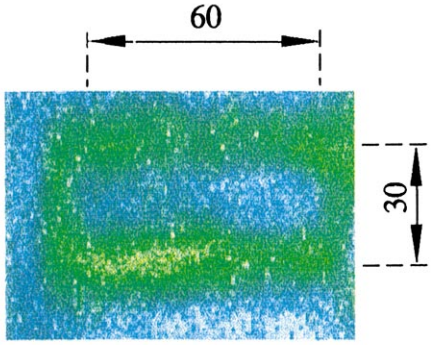

(b)

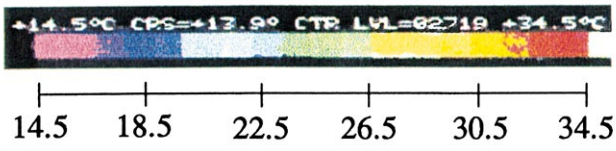

Figure 13. Temperature field on the heated wall (window boundaries are given by - - -), $Fr_L = 0.59$, $Fr_G = 0.19$: (a) the bubble passes the upper part of the pipe; (b) the liquid passes the upper part of the pipe.

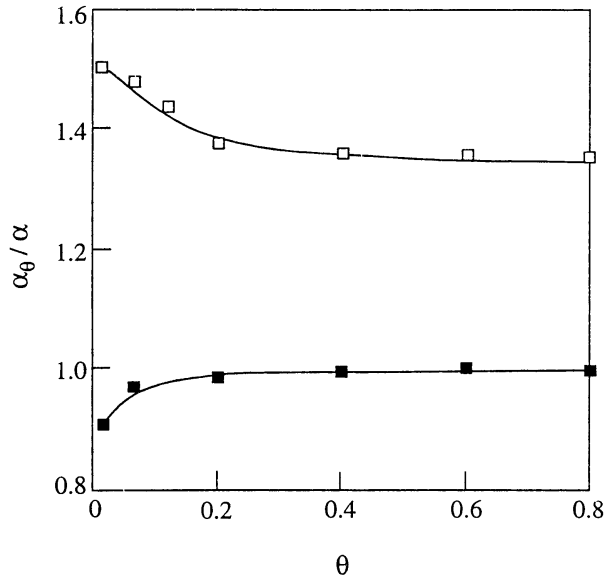

Figure 14. Dimensionless time-average local heat transfer coefficients, $Fr_L = 0.59$, $Fr_G = 0.45$: □, liquid phase; ■, gas phase.

4.3.4. *Heat transfer along the tube*. The dimensionless length of the heating section is $L/D = 3.6$. Therefore, the question arises as to whether this affects the results of heat transfer. In order to provide an answer, the heat transfer coefficients on top of the tube were obtained at different locations along the tube. The measurements were carried out at an angle of inclination of 2°. The distances from the entrance of the heating section to the measuring points were $x/D = 0.4$, 0.9, 1.8 and 2.4. For each flow condition, the measurements were repeated at least three times. In the single-phase water flow the measurements were carried out for the average water velocities $U_{L1} = 0.40$ and $U_{L2} = 0.82$ m/s. The heat transfer coefficients α_0, obtained in these experiments, agree with calculations carried out using the k–ε model. Then, the results were compared with the heat transfer coefficient α_θ in the air–water flow. The experiments in the two-phase flow were carried out at the same water flow rates, i.e. with the superficial liquid velocities $U_L = 0.40$ m/s ($Fr_L = 0.59$) and $U_L = 0.82$ m/s ($Fr_L = 1.2$). Figure 15(a) shows the ratio of $\alpha_{\theta=0}/\alpha$ vs. x/D at $Fr_L = 0.59$ and the gas Froude numbers $Fr_G = 0.03$ and $Fr_G = 0.19$. Figure 15(b) shows $\alpha_{\theta=0}/\alpha$ vs. x/D at $Fr_L = 1.2$ and $Fr_G = 0.08$ and $Fr_G = 0.33$. Although both α_0 and $\alpha_{\theta=0}$ decrease when x/D increases, the ratio $\alpha_{\theta=0}/\alpha$ does not depend on x/D. For this reason, all results of heat transfer in our study are presented as a ratio of the heat transfer coefficient in a two-phase flow to the one in a liquid-phase flow.

4.4. *Heat transfer on the lower part of the tube*

When the angle $\bar{\theta} > 0.8$, only the liquid-phase was observed on the lower part of the tube. Although this type of flow is significantly simpler than the two-phase flow, analytical models for the heat transfer, from a wall of an inclined tube to the water, do not exist. It may be expected that the treatment presented above for a bubble flow is also applicable for a single-phase flow, i.e. an additional turbulent heat flux is assumed to be subdivided into two components, one due to the inherent liquid turbulence and the other caused by bubble motion. Typical thermal patterns on the wall are shown in figure 16(a,b). The pictures were taken by the IR camera placed under the pipe. In figure 16(a) the flow is a single-phase one, from the right to the left, and the liquid velocity is $U_L = 0.40$ m/s. The temperature field, visualized by the IR radiometer, indicates a streaky pattern that consists of high-temperature streaks (red colour) and low temperature streaks (green colour). Figure 16(b) shows the thermal pattern in air–water flow at liquid velocity $U_{LS} = 0.40$ m/s ($Fr_L = 0.59$), and gas Froude number $Fr_G = 0.33$. This figure is quite different from the previous one and confirms the new nature of the flow pattern. The increase in the heat transfer coefficient is associated with turbulence caused by bubble motion. Under these

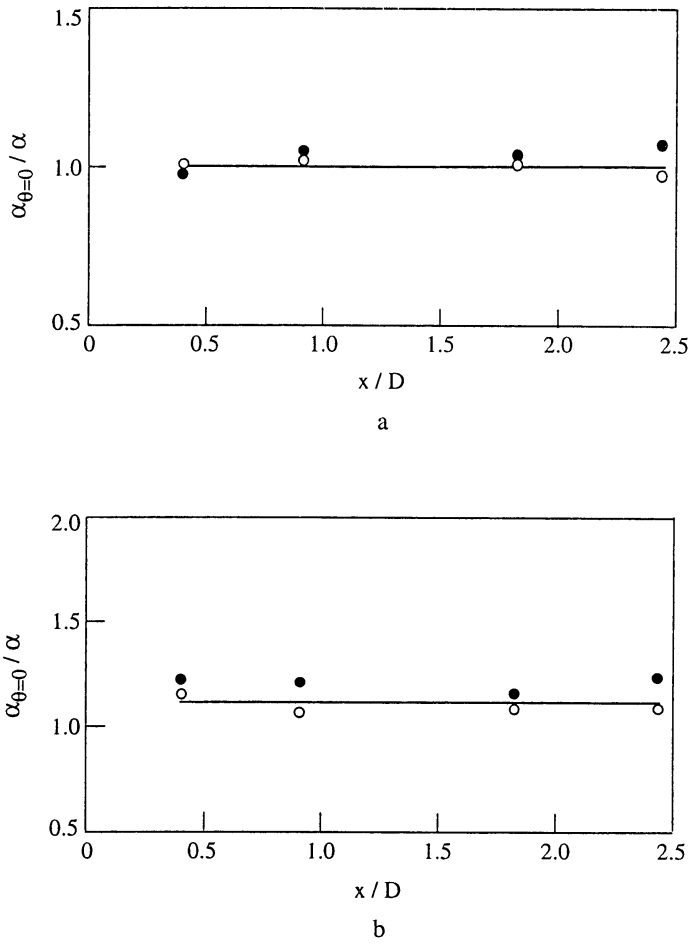

Figure 15. Dimensionless heat transfer coefficient along the top of the pipe (β = 2°): (a) $Fr_L = 0.59$; ○, $Fr_G = 0.03$; ●, $Fr_G = 0.19$; (b) $Fr_L = 1.2$; ○, $Fr_G = 0.08$; ●, $Fr_G = 0.33$.

conditions, the relative time- and space-average heat transfer coefficient

$$\bar{\alpha}_\theta = \frac{1}{\theta_2 - \theta_1} \int_{\theta_1}^{\theta_2} \alpha_\theta \, d\theta$$

increases as

$$\bar{\alpha}_\theta/\alpha = (1 + fL/u_b)^{0.5} \qquad [12]$$

in the range $0.8 \leq \theta \leq 2.0$, $0.03 \leq Fr_G \leq 0.57$, $0.59 \leq Fr_L \leq 2.0$. This relation describes the data with a standard deviation of 9%.

5. DISCUSSION

5.1. *Flow patterns in horizontal and inclined tubes*

The experimental data for heat transfer in air–water flow have usually been correlated according to the hypothesis that the heat transfer depends on the gas and liquid velocities and properties. Furthermore, the heat transfer coefficient depends strongly on the conditions of heating: phase-change effects, mass transfer, compressibility, etc. The heat transfer coefficient in the gas–liquid flow may be correlated by the following methods:

1. analogy between heat transfer and momentum transfer (Hughmark 1965);
2. interrelation between the heat transfer coefficient in a two-phase flow and that in a liquid single-phase flow (Bar-Cohen *et al.* 1987);

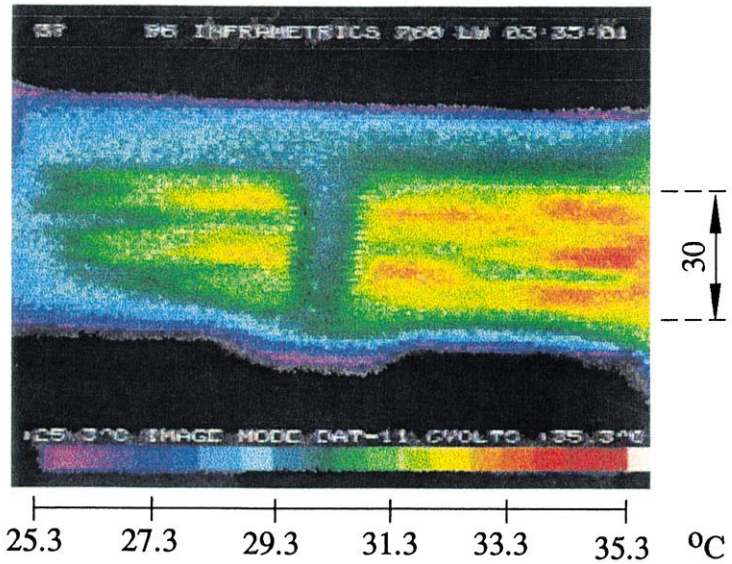

(a)

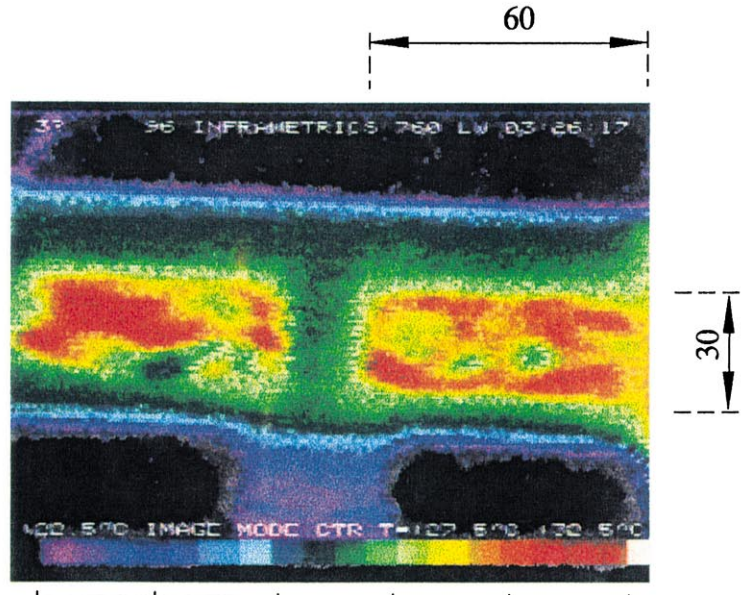

(b)

Figure 16. Thermal pattern on the lower part of the pipe (window boundaries are given by - - -), $Fr_L = 0.59$: (a) $Fr_G = 0.0$; (b) $Fr_G = 0.33$.

3. direct correlation as a function of liquid properties, fluid velocities and other operating conditions (Kago *et al.* 1986).

All these methods assumed a homogeneous air–water flow and cannot be applied to an intermittent flow. In order to clarify the effect of surface orientation on the heat transfer in an intermittent air–water two-phase flow, we consider at first the effect of inclination angle on such parameters as bubble length, height, and frequency.

Figure 17 shows a comparison of $\alpha_{\theta=0}$ for horizontal and inclined tubes. The plot of the heat transfer coefficient vs. the gas Froude number shows that in an inclined tube the heat transfer coefficient is much higher, compared with that for a horizontal tube. The effect of surface orientation may be explained if the heat transfer is related to the flow pattern. We believe that the parameter fL/u_b reflects the approximate relation between flow regimes in horizontal and inclined tubes and the heat transfer mechanism. A typical behaviour of fL/u_b in horizontal and inclined tubes ($\beta = 5°$) is shown in figure 18, where its values are plotted vs. the air Froude number, Fr_G, at a constant value of the water Froude number, $Fr_L = 1.2$.

All the data for horizontal and inclined tubes is summarized in table 3. It can be seen that the magnitude of fL/u_b for all flow regimes studied in a horizontal tube is much larger than that in an inclined tube. Since this parameter reflects the ratio of the time occupied by air to the total residence time of a two-phase mixture on the heated wall, the heat transfer in a horizontal tube is, generally, drastically reduced compared to that in an inclined tube. This phenomenon has been studied in detail and the results are considered below.

Figure 19 indicates that for an inclined tube the average bubble length is smaller than that in a horizontal tube. The appearance and motion of large elongated bubbles lead to a decrease in the heat transfer coefficient.

In an inclined tube, both the bubble velocity and height have magnitudes significantly higher than those in a horizontal tube. This can be shown by comparison between the data for inclined and horizontal tubes presented in figures 20 and 21. The dimensionless bubble velocity and height have been plotted vs. the air Froude number, at $Fr_L = 1.2$. As a consequence, the heat

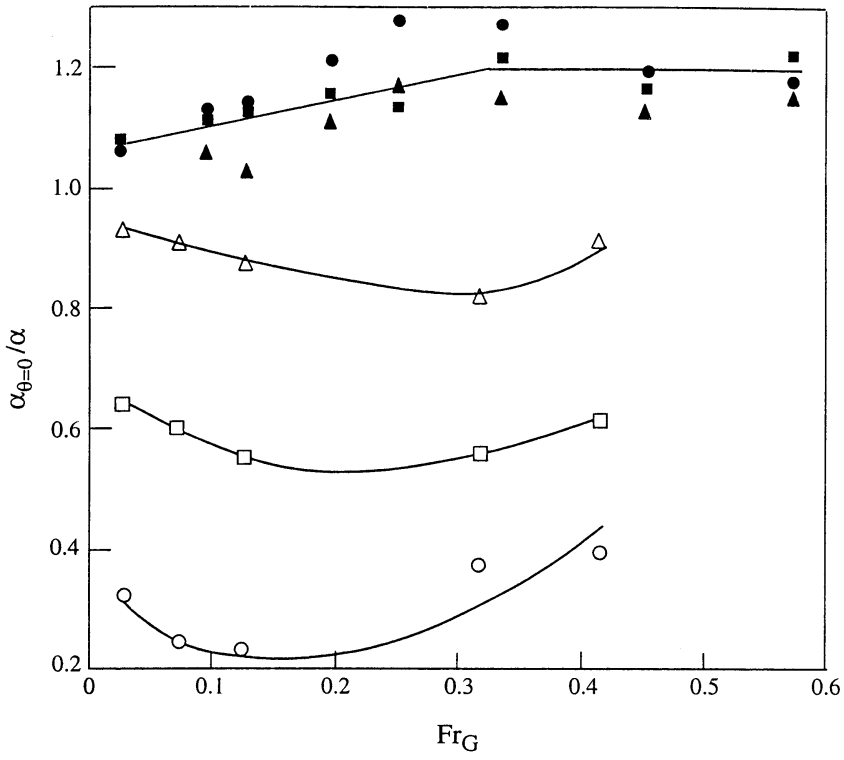

Figure 17. Heat transfer coefficients at the top of horizontal and inclined tubes: Horizontal - ○, $Fr_L = 0.59$; □, $Fr_L = 1.2$; △, $Fr_L = 2.0$; Inclined with $\beta = 5°$ – ●, $Fr_L = 0.59$; ■, $Fr_L = 1.2$; ▲, $Fr_L = 2.0$.

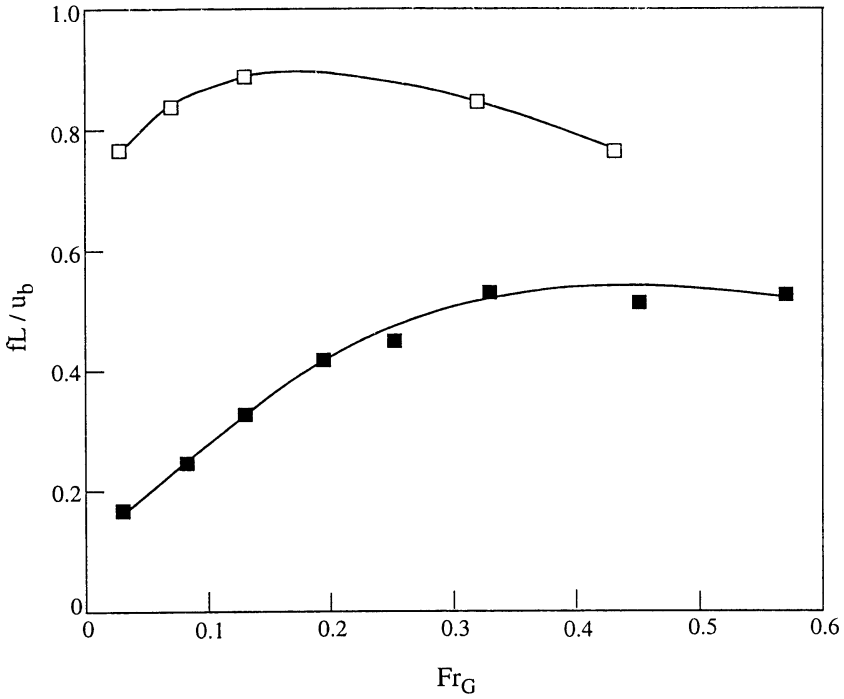

Figure 18. Dependence of fL/u_b on gas Froude number for the horizontal and inclined tube, $Fr_L = 1.2$; □, horizontal tube; ■, inclined tube ($\beta = 5^\circ$).

transfer coefficient becomes large when bubble velocity and height increase. We believe that the bubble motion parameters should receive considerable attention because of their fundamental importance for the intermittent flow pattern. The front of the bubble disturbs the liquid; the tail produces vortex motion. This phenomenon is different for the flow in horizontal and inclined tubes, and its effect on the heat transfer depends on the gas Froude number.

Table 3. Flow parameter fL/u_b for horizontal and inclined tubes

Flow in the horizontal tube			Flow in the inclined tube, $\beta = 5^\circ$		
Liquid Froude number Fr_L	Gas Froude number Fr_G	Flow parameter fL/u_b	Liquid Froude number Fr_L	Gas Froude number Fr_G	Flow parameter fL/u_b
0.90	0.03	0.78	0.59	0.03	0.15
	0.07	0.82		0.08	0.31
	0.13	0.93		0.13	0.36
	0.32	0.88		0.19	0.47
	0.43	0.74		0.25	0.48
				0.33	0.46
				0.45	0.52
				0.57	0.60
1.3	0.03	0.76	1.2	0.03	0.16
	0.07	0.84		0.08	0.25
	0.13	0.88		0.13	0.32
	0.32	0.85		0.19	0.41
	0.43	0.76		0.25	0.44
				0.33	0.54
				0.45	0.51
				0.57	0.53
2.0	0.03	0.88	2.0		
	0.07	0.86			
	0.13	0.95		0.13	0.31
	0.32	0.91		0.19	0.31
	0.43	0.84		0.25	0.36
				0.33	0.42
				0.45	0.49
				0.57	0.53

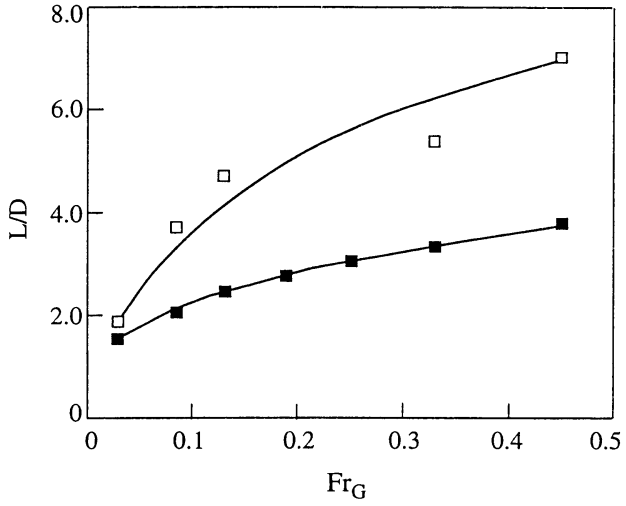

Figure 19. Dependence of dimensionless bubble length on gas Froude number for horizontal and inclined tube, $Fr_L = 1.2$; □, horizontal tube; ■, inclined tube ($\beta = 5°$).

Data in the literature, on the local heat transfer around the circumference of a pipe with a two-phase intermittent non-adiabatic flow, describe horizontal pipes only. The main concern is determination of the wall dryout. Different types of dryout may occur, depending on gas and liquid superficial velocities. At the low gas and liquid superficial velocities, stratified flow dryout yields high temperature differences between the top and bottom of the pipe. As the liquid velocity increases, the wall temperature is determined by a so-called intermittent flow dryout. Crowe and Griffith (1993) showed that waves and slugs cool down the top of the pipe. In the present study, such characteristics as the liquid Froude number and flow parameter fL/u_b have been found to affect the dryout and local heat transfer in the horizontal pipe.

The poor heat transfer may be avoided if the tube is slightly inclined. In this case, an increase in gas velocity may lead to the transition region. The latter exists where a liquid film at the top of the pipe is gradually built up. In the present study, visual observations through the glass pipe enabled us to distinguish different flow details, but we did not observe this phenomenon.

In the inclined air–water flow, bubbles present a fluctuating motion which is partly related to the random motion of the continuous-phase. This 'turbulent' motion is responsible for the dispersion of small bubbles, and thus presents one of the basic mechanisms which control the heat transfer on the upper part of the tube.

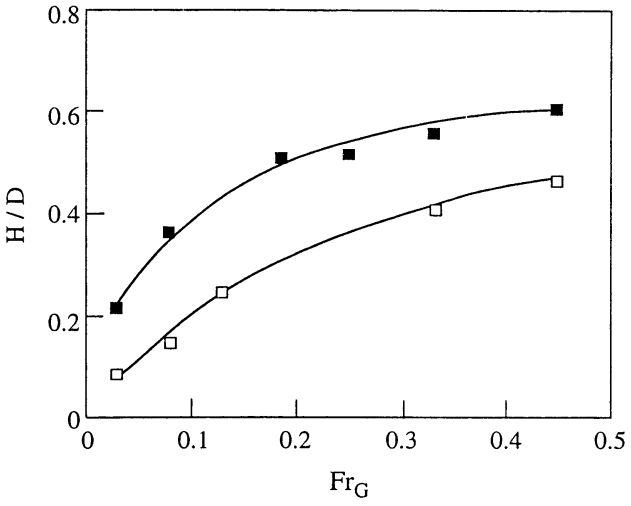

Figure 20. Dependence of dimensionless bubble height on gas Froude number for horizontal and inclined tube, $Fr_L = 1.2$; □, horizontal tube; ■, inclined tube ($\beta = 5°$).

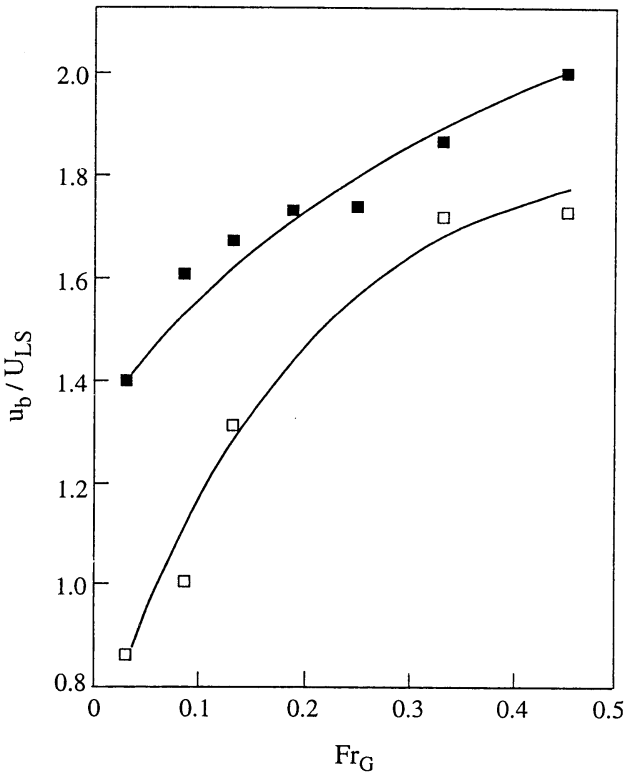

Figure 21. Dependence of dimensionless bubble velocity on gas Froude number for horizontal and inclined tube, $Fr_L = 1.4$; □, horizontal tube; ■, inclined tube ($\beta = 5°$).

5.2. *Heat transfer in horizontal and inclined tubes at low gas Froude number*

One of the surprising features of the heat transfer for horizontal and inclined tubes is the behaviour of the dimensionless heat transfer coefficient at $0 \leq \theta \leq 0.17$ and low gas Froude numbers. In the range $0.03 \leq Fr_G < 0.14$, the parameter fL/u_b increases both in horizontal and inclined tubes. However, under these conditions the heat transfer coefficient in a horizontal tube decreases, in contrast to the coefficient in an inclined tube. Thus, the dependence of the heat transfer coefficient on fL/u_b is rather different for horizontal and inclined tubes, and is discussed below.

Consider [6] for a flow in a horizontal tube. In this case the heat transfer mechanism is characterized by an intermittent appearance of elongated bubbles that move slowly along the top of the pipe. Assuming that the air-phase heat transfer coefficient is much smaller than that for the liquid-phase, [6] can be written as follows:

$$\frac{\alpha_\theta}{\alpha} = \frac{\alpha_s}{\alpha}\left(1 - \frac{fL}{u_b}\right). \qquad [13]$$

According to [13], in a horizontal tube, the heat transfer coefficient decreases when fL/u_b increases. For an inclined tube the heat transfer coefficient is mainly controlled by the stirring action of bubbles.

The turbulent dispersion plays an important role in increasing the heat transfer. The experiments carried out in the present study show that this effect is more pronounced at low gas and liquid Froude numbers.

In the single-phase flow along the heated wall, thermal streaks were observed. When the air–water mixture flows along the inclined heated surface at low air Froude numbers, an increase in Fr_G leads to an increase in the heat transfer coefficient on the upper part of the heated surface.

The presence of gas-phase introduces permanent perturbations into the liquid flow. This may result in the development of the bubble-induced turbulent structures. Karabelas and Hanratty (1968) showed that at the superficial liquid velocities of $U_{LS} > 0.15$, the ratio of the wall shear

stress with the bubbles to the nominal value, τ_{wb}/τ_w, is larger than unity. The slope of the velocity profile becomes smaller than that predicted by the law of the wall for a single-phase liquid. This conclusion is supported by the recent study of Kashinsky and Timkin (1997). Since the heat transfer coefficient is connected to the shear stress, it should increase. Thus, the enhancement of the heat transfer may be related to the bubble-induced turbulence.

The bubble-induced turbulence phenomenon was also found by Liu and Bankoff (1993) in a vertical pipe. The present study shows that in this regime the temperature of the upper part of the heated surface is actually less than that of the lower part, even when the bubbles of air pass along the upper part, see figure 14. This interesting phenomenon was found for the inclined tube at all liquid Froude numbers.

6. CONCLUSIONS

In order to clarify the effect of pipe inclination on the two-phase heat transfer, experiments were carried out for an air–water flow at atmospheric pressure. The inclination angle of a heated tube varied from 2° to 5°.

It was found that the heat transfer in an inclined tube is, generally, drastically enhanced compared to that in a horizontal one. In order to understand this phenomenon, the data on the circumferential temperature distribution in horizontal and inclined tubes was collected and analysed. The analysis revealed the importance of the hydrodynamic phenomena for the heat transfer. Attention was concentrated on such characteristics of the intermittent flow as bubble size, velocity, and frequency. A dependence of the local heat transfer on these parameters of the flow pattern was established.

A two-phase heat transfer mechanism was proposed, based on a physical model. It was shown that this mechanism can be related to bubble geometry and motion parameters. Two different mechanisms of heat transfer were discussed: one accounts for the heat transfer due to replacement of the liquid layer by an elongated bubble passing along the surface; the other is due to the additional turbulence caused by the bubbles. The analysis indicated that the heat transfer from a horizontal tube is controlled mainly by the thermal layer formed on the wall by an elongated air bubble. The bubble-induced turbulence affects mainly the heat transfer in inclined tubes.

Acknowledgements—This research was supported both by the Basic Research Foundation administered by the Israeli Academy of Sciences and Humanities, by a grant from the NCRC and the Forschungszentrum Jülich GMBH (KFA), and by the Fund of Promotion of Research at the Technion. Baigeng Hu was supported by a Lady Davis Postdoctoral Fellowship. Jinghai Yi was supported by an Israel Higher Education Council Postdoctoral Fellowship. A. Mosyak was partially supported by the Center for Absorption in Sciences, Ministry of Immigrant Absorption (State of Israel).

REFERENCES

Bar-Cohen, A., Ruder, Z. and Griffith, P. (1987) Thermal and hydrodynamic phenomena in a horizontal, uniformly heated steam generating pipe. *J. Heat Transfer, Trans. ASME* **109,** 739–745.

Barnea, D., Shoham, O., Taitel, Y. and Dukler, A. I. (1980) Flow pattern transition for horizontal and inclined pipes: Experimental and comparison with theory. *Int. J. Multiphase Flow* **6,** 217–225.

Barnea, D. and Taitel, Y. (1986) Flow pattern transition in two-phase gas–liquid flows. *Encyclopedia of Fluid Mechanics*, ed. N. P. Cheremisinoff, pp. 403–474. Houston Publishing, Gulf, TX.

Bogdanov, V. V. (1955) Investigation of the effect of the rate of the motion of the water current on the heat exchange coefficient on boiling in inclined tube. *Izvestiya Akademii Nauk, Otdelenie Technicheskikh Nauk* **4,** 136–140 (in Russian); *AERE Lig./Trans.* 596.

Creutz, M. (1994) Experimental and theoretical studies on unclosed annular two phase flow in slightly inclined pipes. *Direct Solar Steam in Parabolic Trough Collectors*, ed. M. Muller. Plataforma Solar de Almeria, Almeria, Spain.

Creutz, M., Taitel, Y., Barnea, D., Muller, M. and Mewes, D. (1995) The transition region between intermittent, stratified and annular two-phase flow in upward inclined pipes. *33rd European Two-phase Flow Group Meeting*.

Crowe, K. E. and Griffith, P. (1993) Intermittent flow dryout limit in heated horizontal tubes. *Int. J. Multiphase Flow* **19,** 575–588.

Dorresteijn, W. R. (1970) Experimental study of heat transfer in upward and downward two-phase flow of air and oil through 70 mm tubes. *Proc. 4th Int. Heat Transfer Conference*, Vol. V, B5.9. Elsevier, Amsterdam.

Elamvaluthi, G. and Srinivas, N. S. (1984) Two-phase heat transfer in two component vertical flows. *Int. J. Multiphase Flow* **10,** 237–242.

Gilli, P. R. (1963) *Forschung auf dem Gebiet der Fallfilverdampfung*, Vol. 86S, pp. 288–300. VGB-Mitteilungen.

Hughmark, G. A. (1965) Hold-up and heat transfer in horizontal slug gas–liquid flow. *Chem. Eng. Sci.* **20,** 1007–1010.

Kago, T., Saruwatari, T., Kashima, M., Morooka, S. and Kato, Y. (1986) Heat transfer in horizontal plug and slug flow for gas–liquid and gas–slurry systems. *J. Chem. Eng. Jpn* **19,** 125–131.

Karabelas, A. J. and Hanratty, T. J. (1968) Determination of the direction of surface velocity gradients in three-dimensional boundary layers. *J. Fluid Mech.* **34,** 159–162.

Kashinsky, O. N. and Timkin, L. S. (1997) Development of pseudo-turbulent structure in upward bubbly flow. *Proc. 4th World Conference on Experimental Heat Transfer, Fluid Mechanics and Thermodynamics*, Brussels, 2–6 June, eds M. Giot, F. Mayinger, G. P. Celata. Edizioni ETS, Pisa.

Krishna, M. and Rao, D. P. (1985) Studies on flow boiling in an inclined tube with reference to solar collectors. INTERSOL 85. *Proc. 9th Biennial Congress of the Int. Solar Energy Society*, Vol. 2, pp. 1368–1372. Pergamon Press, New York.

Lin, P. Y. and Hanratty, T. J. (1987) Effect of pipe diameter on flow patterns for air–water flow in horizontal pipes. *Int. J. Multiphase Flow* **13,** 549–563.

Liu, T. J. and Bankoff, S. G. (1993) Structure of air–water bubble flow in a vertical pipe—I. Liquid mean velocity and turbulence measurements. *Int. J. Heat Mass Transfer* **36,** 1049–1060.

Muller, M. (1993) How to master the DSG process? Some open questions. *Proc. 5th Sde Boker Symposium on Solar Electricity Production*, Israel, pp. 203–235.

Muller, M. (1995) Stromungsphanomene bei der Direktverdampfung in Parabolrinnen-Solarkraftwerden, Dissertation, Universität Munchen.

Shoham, O., Dukler, A. E. and Taitel, Y. (1982) Heat transfer during intermittent/slug flow in horizontal tubes. *Ind. Eng. Chem. Fundam.* **21,** 312–318.

Singh, G. and Griffith, P. (1970) Determination of the pressure drop optimum pipe size for a two-phase slug flow in an inclined pipe. *J. Eng. Ind., Trans. ASME* **92,** 717–726.

Taitel, Y. and Dukler, A. E. (1976) A model for predicting flow regime transitions in horizontal and near horizontal gas–liquid flows. *AIChE Journal* **22,** 47–55.

Weisman, J. and Kang, S. Y. (1981) Flow pattern transitions in vertical and upwardly inclined lines. *Int. J. Multiphase Flow* **7,** 721–729.

Zukoski, E. E. (1966) Influence of viscosity, surface tension, and inclination angle on motion of long bubbles in closed tubes. *J. Fluid Mech.* **25,** 821–837.